J. Fluid Mech. (1983), *vol.* 127, *pp.* 299–313
Printed in Great Britain

Rotating compressible flows with internal sources and sinks

By HOUSTON G. WOOD
Department of Mechanical and Aerospace Engineering, University of Virginia, Charlottesville

AND G. SANDERS
Oak Ridge Gaseous Diffusion Plant, Union Carbide Corporation, Nuclear Division, Oak Ridge, Tennessee

(Received 5 March 1981 and in revised form 9 August 1982)

An analysis is presented that describes a model of the flow field of a rotating compressible fluid in a cylinder with internal sources or sinks of mass, momentum or energy. A solution of the mathematical model is obtained using an expansion in eigenfunctions of the corresponding homogeneous equation. The internal sources or sinks produce countercurrent flows analogous to flows generated by boundary conditions in the classical analysis of the problem. The application of this model to the flow driven by a feed stream or a scoop is discussed. Some sample calculations are presented that illustrate the countercurrent flow produced by sources of mass, the three components of momentum, energy and a mass source/sink combination. Calculations simulating feed introduction and a tails-removal scoop have been performed and the fluid-dynamics solutions have been used to calculate the optimum separative performance of the example centrifuge.

1. Introduction

The gas centrifuge is an object of much interest for the purpose of producing uranium enriched in the fissionable isotope ^{235}U to be used as fuel for nuclear power reactors. The papers of Hoglund, Shacter & Von Halle (1979), Soubbaramayer (1979) and Olander (1972) provide a very good introduction to the theory of isotope separation by the gas-centrifuge process. The radial pressure gradient produces a separation in which the heavier $^{238}UF_6$ molecule tends to be concentrated near the periphery and the lighter $^{235}UF_6$ molecule tends to be concentrated near the axis. By imposing a countercurrent flow in the axial direction, the separation effect can be greatly enhanced over the simple radial separation.

The primary motion of the gas in the cylinder at a uniform temperature is to rotate with the cylinder as though the gas were a solid filling the hollow cylinder. This primary motion is referred to as solid-body isothermal rotation. The density and pressure gradients are exponentially decaying functions towards the axis. A number of disturbing mechanisms lead to a secondary flow which has an axial countercurrent circulatory motion. The countercurrent flow is induced by temperature gradients on the cylinder boundaries, by the presence of stationary scoops for mass removal, and by the injection and removal of mass. Figure 1 depicts a configuration that has frequently been analysed in the literature (Soubbaramayer 1979).

The separative work produced by a centrifuge has been considered by Park (1981), who analysed the isotope distribution and separative work without any analysis of

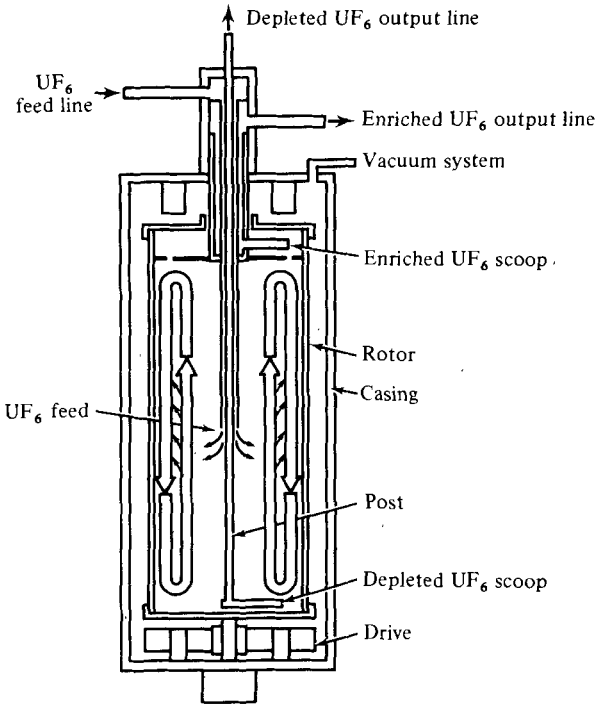

FIGURE 1. Gas centrifuge.

the underlying fluid dynamics. Soubbaramayer & Billet (1980) have presented an analysis of both the fluid dynamics and the isotope separation in which the countercurrent flow mechanisms considered include a temperature gradient along the rotor wall, elevated temperatures on the two end caps, and a bottom end cap that is rotating at a slightly different frequency than the vertical wall of the rotor. The differentially rotating end cap is intended to simulate the action of the stationary bottom scoop shown in figure 1. The countercurrent flow induced by the injection of mass from the centre post has not been taken into account.

Wood & Morton (1980) have presented an analysis that allows the calculation of countercurrent flows induced by sources or sinks of mass, momentum and energy that are interior to the rotating gas rather than on the boundaries of the cylinder. In this paper we will demonstrate how the sources and sinks can be used to simulate flows that can be attributed to scoops and mass injection.

2. Fluid-dynamics model

We will use the same notation as given in Wood & Morton (1980). The system of equations governing the flow are combined to give the non-homogeneous form of Onsager's pancake equation, which is

$$(e^x(e^x\chi_{xx})_{xx})_{xx} + B^2\chi_{yy} = F(x, y), \tag{2.1}$$

where

$$F(x, y) = \frac{B^2A^2}{2\,Re\,S}\int_x^\infty (T_y - 2V_y)\,dx' - \frac{B^2}{4A^4}\int_x^\infty \int_0^{x'} M_y\,dx''\,dx'$$

$$- \frac{B^2A^2}{2\,Re\,S}[(e^xU_y)_x + (e^xW)_{xx}]. \tag{2.2}$$

The function χ is a potential function whose derivatives yield the primitive variables u, v, w, ρ and T. The radial variable x counts density scale heights from the rotor wall and is related to the radius by $x = A^2[1-(r/a)^2]$. The axial variable is $y = z/a$, where a is the radius. The speed parameter is $A^2 = MV^2/2RT$, where M is molecular weight, V is peripheral speed, R is the universal gas constant and T is the temperature. The parameter

$$S = 1+\frac{\gamma-1}{2\gamma}Pr\,A^2,$$

where γ is the ratio of specific heats and Pr is the Prandtl number. The number $Re = \rho_w Va/\mu$, where ρ_w is the density at the wall and μ is the viscosity. The parameter B is then defined as $B = Re\,S^{\frac{1}{2}}/4A^6$. The non-homogeneous part of (2.1) contains the internal source terms for sources or sinks of mass M, momentum (U, V, W) and internal energy T.

In order to determine the countercurrent flow, (2.1) must be solved. For the homogeneous case, the mathematical details of the solution technique by eigenfunction expansions have been described by Wood & Morton (1980), and a solution by finite elements for the homogeneous case has been given by Gunzburger & Wood (1980). A method for solving the non-homogeneous form of (2.1) with eigenfunctions is presented in §3.

The source distribution and strength can be estimated for the feed injection and the tails-withdrawal scoop by separate analyses. An idealized model of how the feed gas injected from the centre post interacts with the rotating gas can be constructed by making some simplifying assumptions. First, we assume that the feed gas leaves the centre post in an azimuthally symmetric manner and that it is not rotating relative to the laboratory reference frame. Secondly, we assume that the feed gas is indistinguishable from the rotating gas after one collision, and that this collision occurs at the radial position where the mean free path is equal to a local density scale height. When the gas exits the hole in the feed pipe, it enters a vacuum and should undergo cooling due to the expansion and should spread in the axial direction before colliding with the rotating gas. Thirdly, for this idealized model, we assume that when the feed gas reaches the collision location it has the same temperature as the mean temperature of the rotating gas. Fourthly, we assume a shape function for the axial spreading. The mathematical description of the source terms can then be given as

$$S(x,\,y) = S_0\,G(x)\,H(y), \tag{2.3}$$

where S_0 is the strength, $H(y)$ is the axial distribution and $G(x)$ is the radial distribution. These functions are then used in the right-hand side of (2.2) in order to prescribe the non-homogeneous part of (2.1).

With these assumptions, the feed can be modelled as a source of mass whose strength can be determined from the feed rate $\dot{m}$ to the machine. The source of mass will induce a non-homogeneous term in the vector form of the Navier–Stokes equation, which will be treated as an effective sink. The simplifying assumptions above lead us to hypothesize a feed-gas velocity vector with only one non-zero component u_f, which is in the radial direction. Therefore the radial momentum equation will have a source of strength $\dot{m}u_f$ and the azimuthal momentum equation will have an effective sink of strength $-\dot{m}\Omega r_f$, where r_f is the radial location of the collision between the feed gas and the rotating gas. Also, owing to the source of mass, an effective source of internal energy will be induced with a strength given by $\frac{1}{2}\dot{m}[(\Omega r_f)^2+u_f^2]$.

Now the scoop is fundamentally different from the feed, since it imposes a drag on the gas whether or not mass is being removed. The drag is simply a sink of angular momentum, whose strength we will denote by $-f$, and a non-homogeneous term $f(\Omega r_f)$ will appear as an effective source in the internal energy equation. The value of f can be determined from an independent analysis of the scoop geometry or from an analysis to optimize the separative performance. The scoop will also act as a sink of mass, whose strength is given by the tails-removal rate.

3. Solution of the non-homogeneous equation

The solution to (2.1) can be written as

$$\chi = \chi_c + \chi_p, \tag{3.1}$$

where χ_c is the characteristic solution for the homogeneous equation and χ_p is the particular solution. In Wood & Morton (1980) (hereinafter referred to as WM), the characteristic solution was obtained using separation of variables and obtaining eigenfunctions corresponding to the cases where the eigenvalue is real, purely imaginary or zero. The sum of these three cases forms a characteristic solution capable of incorporating all combinations of boundary conditions of interest.

We will obtain a particular solution based on an expansion using the end-driven eigenfunctions $f_n(x)$ presented in WM. These eigenfunctions satisfy homogeneous boundary conditions at the rotor wall and at the axis and form a complete orthonormal set. We therefore seek a particular solution

$$\chi_p(x, y) = \sum_{n=1}^{\infty} a_n f_n(x) g_n(y), \tag{3.2}$$

where the coefficients a_n and the function $g_n(y)$ are to be determined from the source distributions and shapes. In practice we have used only the first ten terms of this series. Substituting this expression into (2.1) and denoting the sixth-order differential operator by L, we have

$$L\chi_p + B^2\chi_{pyy} = \sum_{n=1}^{\infty} a_n B^2 f_n(x)\,[-\alpha_n^2 g_n(y) + g_n''(y)] = F(x, y). \tag{3.3}$$

We have used the fact that the eigenfunctions satisfy the differential equation $Lf_n = -\alpha_n^2 B^2 f_n$.

For this method of solution by eigenfunction expansion, only sources of the form

$$S(x, y) = S_0 G(x) H(y) \tag{3.4}$$

will be considered. Thus, if each of the five types of source is treated separately, $F(x, y)$ has the form

$$F(x, y) = F_0 \sigma(x) \eta(y). \tag{3.5}$$

From (2.2) we see that each source type must undergo certain integration or differentiation operations to yield $\sigma(x)$ and $\eta(y)$. For illustration, consider a source of axial momentum W that has the form of (3.4). Then, the non-homogeneous term is given by

$$\begin{aligned} F(x, y) &= -\frac{B^2 A^2}{2\,Re\,S}(e^x W)_{xx} \\ &= -\frac{B^2 A^2}{2\,Re\,S}[(e^x S_0 G(x) H(y))_{xx}] \\ &= -\frac{B^2 A^2}{2\,Re\,S}[S_0 H(y)\,(e^x G(x))_{xx}]. \end{aligned} \tag{3.6}$$

Comparing this expression with (3.5) gives

$$F_0 = -\left(\frac{B^2A^2}{2\,Re\,S}\right)S_0, \quad H(y) = \eta(y), \quad \sigma(x) = (e^x G(x))_{xx}.$$

To obtain the particular solution, we use (3.3) and (3.5) to write

$$\sum_{n=1}^{\infty} a_n B^2 f_n(x)\,[g_n''(y) - \alpha_n^2\, g_n(y)] = F_0\,\sigma(x)\,\eta(y). \tag{3.7}$$

Using the orthonormality of the $f_n(x)$, we have

$$a_n[g_n''(y) - \alpha_n^2\, g_n(y)] = \frac{F_0}{B^2}\eta(y)\int_0^{\infty} f_n(x)\,\sigma(x)\,dx. \tag{3.8}$$

Setting this equation equal to $2a_n\,\eta(y)$, we have

$$g_n''(y) - \alpha_n^2\, g_n(y) = 2\eta(y), \tag{3.9}$$

$$a_n = \frac{F_0}{2B^2}\int_0^{\infty} f_n(x)\,\sigma(x)\,dx. \tag{3.10}$$

Equation (3.9) can be solved by variation of parameters to obtain

$$g_n(y) = -\frac{1}{\alpha_n}\int_0^{y_0} \eta(t)\,e^{-\alpha_n|t-y|}\,dt. \tag{3.11}$$

The coefficients a_n can be determined directly from (3.10) using numerical quadrature. Alternatively, since (3.10) implies

$$\sum_{n=1}^{\infty} a_n f_n(x) = \frac{F_0}{2B^2}\sigma(x), \tag{3.12}$$

the a_n can be determined by applying linear least-squares to the truncated series. We see that the particular solution as expressed by (3.2) satisfies homogeneous lateral boundary conditions. However, χ_{p} makes a contribution to the Ekman boundary conditions and must be included in the determination of the coefficients for the end-driven eigenfunctions, which requires a minor modification of the analysis given in WM. In equations (6.25) and (6.26) of WM, $R_0(x)$ and $R_{y_0}(x)$ are defined in terms of $\chi^* = \chi_0 + \chi_{\mathrm{L}}$, which is the contribution of the characteristic solution formed from the zero-eigenvalue solution and the pure-imaginary-eigenvalue solution. For the non-homogeneous case involving sources and sinks, χ^* must simply be defined as $\chi^* = \chi_0 + \chi_{\mathrm{L}} + \chi_{\mathrm{p}}$.

4. Separation analysis

The formulation of the isotopic-concentration gradient in the axial direction (z-direction) due to Onsager and Cohen and reported in Furry, Jones & Onsager (1939) and Cohen (1951) has often been used for predicting the separative performance of centrifuges in which the overall axial isotopic enrichment is large compared with the radial enrichment. The analysis can be found in many references, such as Hoglund *et al.* (1979), Olander (1972) and Soubbaramayer (1979). The first-order differential equation for the radially averaged concentration $\bar{\xi}$ can be written

$$\left\{\int_0^a \frac{\mathscr{G}^2}{2\pi r c D}dr + \int_0^a 2\pi r c D\,dr\right\}\frac{d\bar{\xi}}{dz} = \left\{\int_0^a -\mathscr{G}\frac{\Delta M\omega^2}{RT}r\,dr\,\bar{\xi}(1-\bar{\xi}) - (\tau - P\bar{\xi})\right\}, \tag{4.1}$$

where the function $\mathscr{G}$ is defined by

$$\mathscr{G}(r,z) = \int_r^a 2\pi r' c w \, dr'$$

and τ is the net axial transport of light isotope, P is the product-removal rate, c is molar density, D is the diffusion coefficient and w is the axial component of velocity. From this gradient equation, the separative performance of the countercurrent gas centrifuge can be readily calculated given the description of the flow within the centrifuge.

Since the model of the flow field is linear, solutions can be formed as linear combinations of other solutions. As demonstrated by Soubbaramayer (1979) and Soubbaramayer & Billet (1980), it is convenient to think of several basic flow fields which can be linearly combined to give a complete flow field. For example, we will consider four basic flow fields:

(i) feed with all material removed through a hole in the top baffle ($\theta = 1$);

(ii) feed with all material removed through the bottom scoop ($\theta = 0$);

(iii) linear wall temperature with end-to-end gradient $\Delta T = 1$ K;

(iv) scoop with momentum sink of 1 dyne.

In (i) and (ii) θ is the cut defined as the product rate divided by the feed rate.

As shown in (4.1) the separation depends on the function $\mathscr{G}$, and each type of drive will have its own $\mathscr{G}$ which we will denote by $\mathscr{G}_k$. Therefore we are interested in

$$\mathscr{G}(r, z) = \sum_{k=1}^{4} d_k \mathscr{G}_k(r, z), \tag{4.2}$$

where the d_k are constants.

From the description of the four flow fields, d_1 and d_2 can be chosen to give any feed rate and cut desired, d_3 will yield the temperature gradient, and d_4 will yield the amount of scoop drive. For example, these constants can be chosen in a manner that will yield the solution of (4.1) that produces the optimum separative work.

5. Computational results

We have attempted to study the secondary flow patterns induced by sources or sinks internal to the flow. In order to simplify the problem we have tried to remove the geometry of the source distribution from the analysis and so we have used idealized distribution functions. From a mathematical-analysis viewpoint, a very useful distribution is provided by the Dirac delta function. However, the discontinuous nature of this function produces Gibb's phenomena when the truncated eigenfunction expansion solution is used unless extra analysis is used. In appendix A a method of smoothing is presented which is easy to apply to this problem and allows the radial dependence of the source function to be provided by a delta function. Therefore in (2.3) we have taken

$$G(x) = \delta(x - x^*), \tag{5.1}$$

where x^* is the radial location of the source. It should be clear that, since the model of the fluid dynamics has assumed that the flow is axisymmetric, the source distribution is a ring in three dimensions.

For the axial distribution, experience has shown that the most prudent way to get smooth numerical results is to use an approximation to the delta function. We have found that a triangle of unit area yields results with only a few terms in the expansion and are much smoother than with a delta function and many more terms. Therefore

the axial source distribution in (2.3) is given by

$$H(y) = \begin{cases} 0 & (|y-y^*| > 0{\cdot}5), \\ -4|y-y^*|+2 & (|y-y^*| \leqslant 0{\cdot}5), \end{cases} \tag{5.2}$$

where y^* is the axial location of the source. In this case $H(y)$ is a triangle of unit base, altitude of 2, and hence unit area. For a centrifuge with large aspect ratio, as we will consider, this function represents a concentrated source.

In order to illustrate the countercurrent flow induced by a source, the centrifuge parameters used by Wood & Morton (1980) are used here. The values are given in table 1 and were obtained from the papers by May (1977) and Durivault & Louvet (1976).

We will present the calculations at only one speed; since the approximations in the hydrodynamic model are less severe at higher speeds, we have chosen 700 m/s. In all cases, ten terms were used in the expansion of the particular solution. Numerical experiments have indicated that the solution is essentially unchanged if four or more terms are used.

The spatial distribution of the axial mass flux provides a measure of the countercurrent flow and is of primary importance for determining separative performance, as we discussed in §4. As is shown in (4.1), the axial mass (or molar) flux defines the function $\mathscr{G}$, which in turn defines the coefficients in the isotope gradient equation. This is discussed in detail in Cohen (1951), Hoglund *et al.* (1979), Olander (1972) and Soubbaramayer (1979). Figures 2(*a–e*) are plots of the axial mass flux as a function of radial position measured in scale heights at the axial location one quarter of the length from the bottom of the rotor. These figures represent the flows driven by source distributions of the form

$$S(x, y) = S_0 G(x) H(y), \tag{5.3}$$

where $G(x)$ is given by (5.1) and $H(y)$ by (5.2), and where $x^* = 8$ and $y^* = \frac{1}{2}y_0$. This choice of (x^*, y^*) is strictly arbitrary. For example, in the case of a centrifuge as shown in figure 1, these coordinates could be determined by the location of the bottom scoop, as we will show later. Calculations are presented for each of the source types to illustrate that a countercurrent flow is predicted.

Figure 2(*a*) represents a source of mass introduced at a rate of 1 g/s with half of the mass removed at each end of the rotor through a hole in the boundary located eight scale heights from the rotor wall. This case is antisymmetric about the axial midplane so the plot at $\frac{3}{4}y_0$ would be the negative of the one presented at $\frac{1}{4}y_0$.

Figures 2(*b–d*) represent sources of radial, angular and axial momentum respectively. Each momentum source has a strength of 1 dyn. The radial- and angular-momentum sources are antisymmetric about the axial midplane, and the axial momentum source is symmetric. The radial-momentum source produces axial fluxes two orders of magnitude less than the other momentum sources. Figure 2(*e*) represents a source of energy with a strength of 1 W. The flow is also antisymmetric about the axial midplane and is identical in shape but opposite in sign to the flow for the angular-momentum source in figure 2(*c*). The relationship between energy and angular-momentum sources is apparent from the form of the non-homogeneity in (2.2).

The four sources that are antisymmetric have been differentiated with respect to the axial variable according to (2.2). Since these source distributions are even functions about the axial midpoint, their derivatives are odd functions and hence the antisymmetric property is not unexpected.

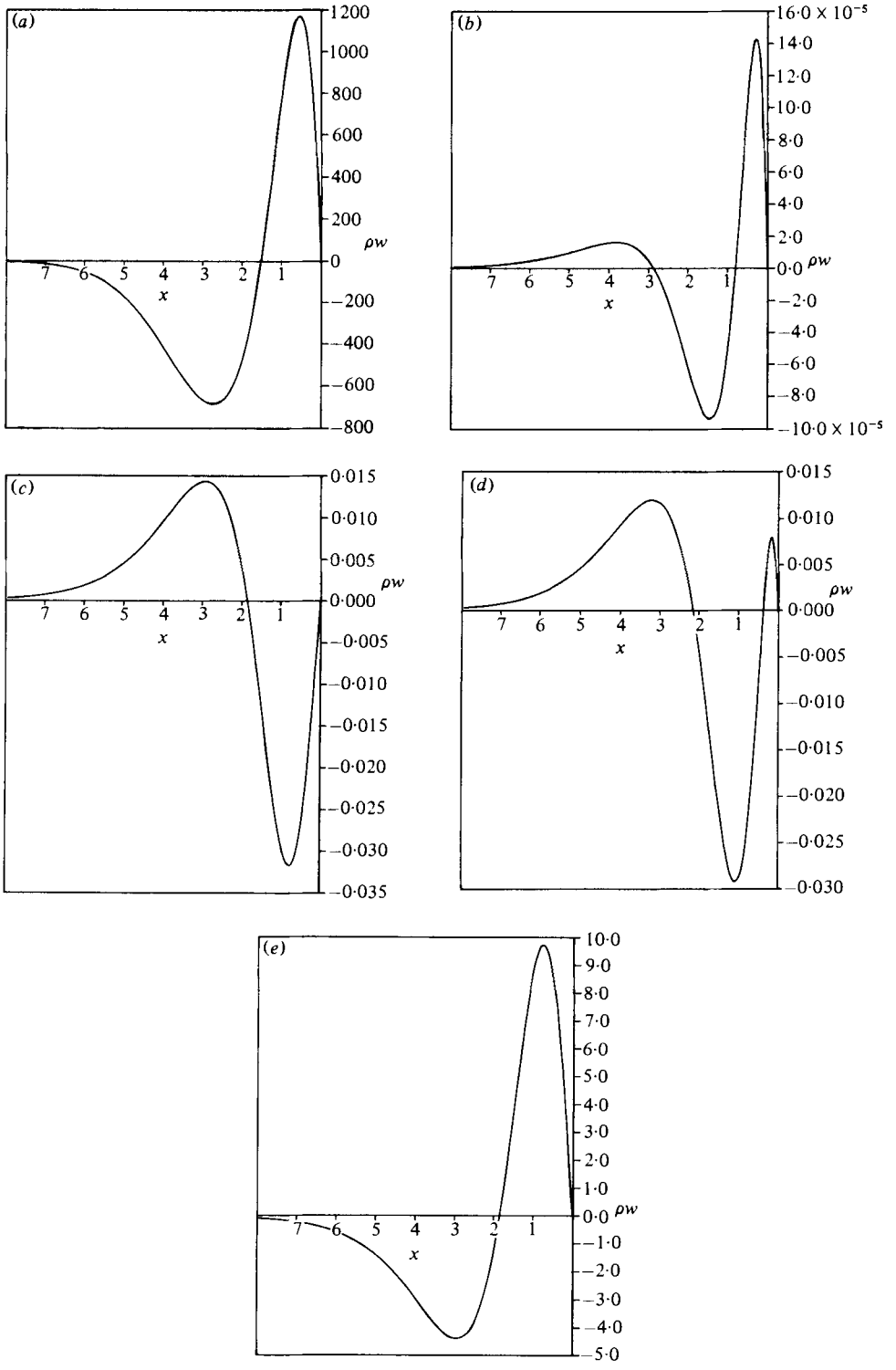

FIGURE 2. Axial mass flux (g/m² s) as a function of scale height at the axial location $\frac{1}{4}y_0$. Flow induced by: (*a*) a mass source of 1 g/s; (*b*) radial-momentum source of 1 dyn; (*c*) azimuthal-momentum source of 1 dyn; (*d*) axial-momentum source of 1 dyn; (*e*) energy source of 1 W; all at $x = 8$, $y = \frac{1}{2}y_0$.

Length	335·3 cm
Radius	9·145 cm
Wall pressure	13·3 kPa (100 torr)
Peripheral speed	400, 500, 700 m/s
Average temperature	300 K

TABLE 1. Centrifuge parameters

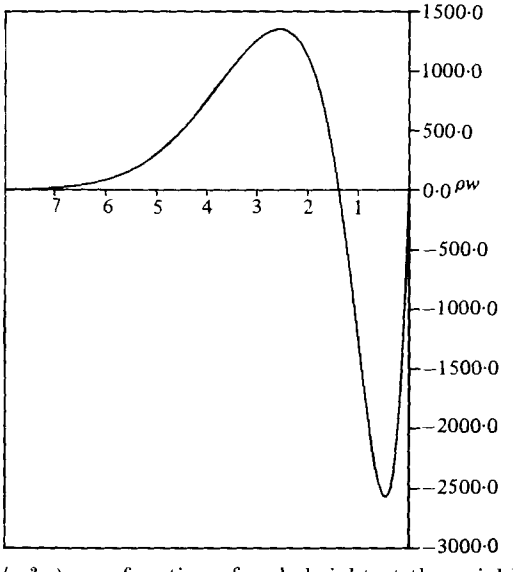

FIGURE 3. Axial mass flux (g/m² s) as a function of scale height at the axial location $\frac{1}{2}y_0$. Flow induced by a mass source of 1 g/s at $x = 8$, $y = \frac{1}{4}y_0$ and a mass sink of 1 g/s at $x = 8$, $y = \frac{3}{4}y_0$.

Figure 3 represents the axial mass flux as a function of scale heights at the axial midplane for a mass source of 1 g/s located at $x^* = 8$ and $y^* = \frac{1}{4}y_0$ and a mass sink of 1 g/s located at $x^* = 8$ and $y^* = \frac{3}{4}y_0$. The shape of the source and sink is the same as that given by (5.3). In this case, no mass is removed through the boundaries.

Figures 4(*a–c*) are contour plots of the streamfunction for the radial-momentum, angular-momentum and axial-momentum sources respectively, that are shown in figures 2(*b–d*). The symmetry of the flow driven by the radial- and the angular-momentum sources is quite clearly demonstrated, as is the antisymmetry of the axial momentum source. The radial-momentum source is very weak and the flow is confined to very near the source. The contour plot of the streamfunction due to an energy source is indistinguishable from that of an angular-momentum source, except that the circulation is reversed.

For the case of mass sources or sinks, a simple analytic form for the streamfunction has not been found. In this case the streamline plots have to be generated from the velocity field and so far we have been unable to generate acceptably accurate plots.

Figure 5 represents the streamlines for flow induced by the presence of a sink of angular momentum located at $x = 4$ and $y = 0{\cdot}25$. The direction of the flow is downwards near $x = 0$, which corresponds to the rotor wall. This case simulates the flow generated by the presence of a stationary bottom scoop at the given location.

The feed and scoop were modelled in the manner discussed in §2, and it was assumed that the feed-induction process was such that the feed velocity was the sound

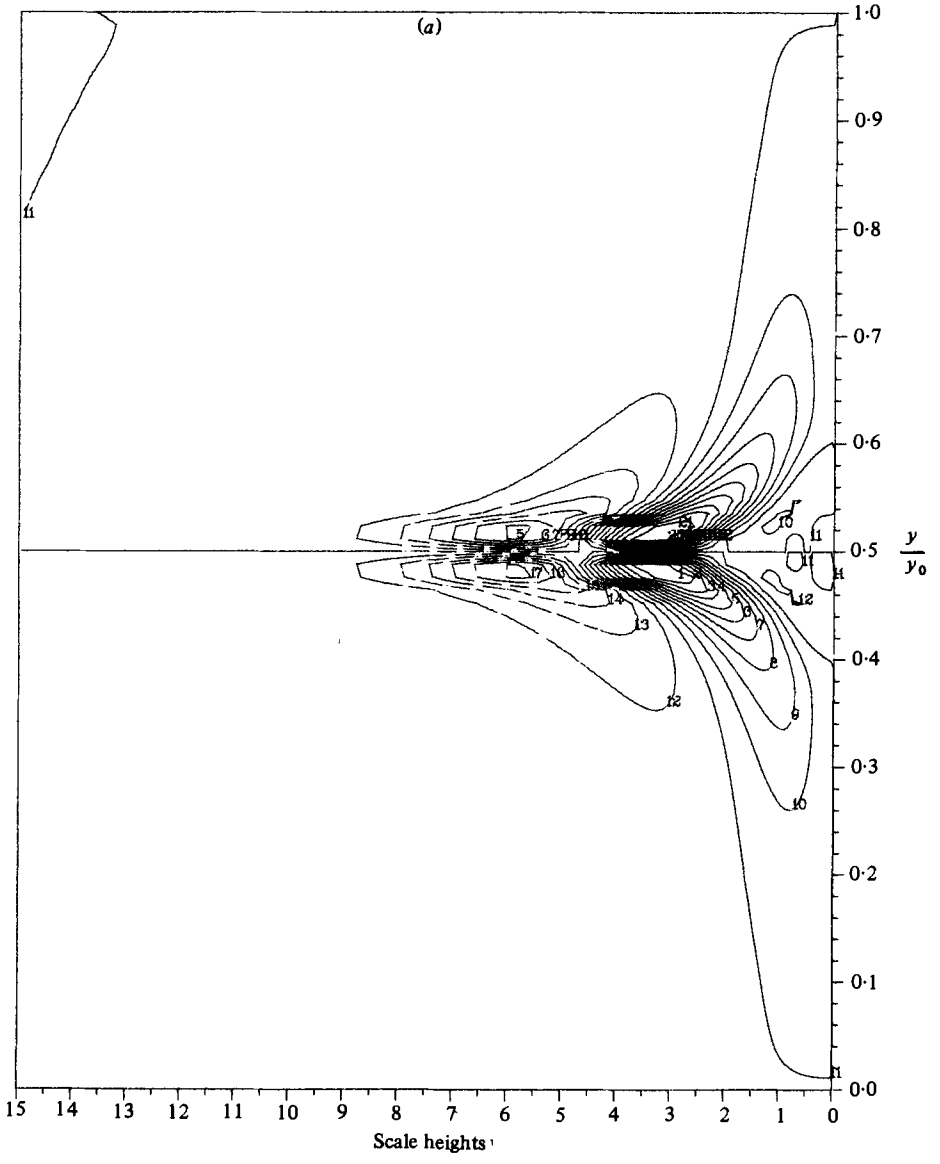

FIGURE 4(a). For caption see p. 310.

speed at the average temperature, i.e. $u_t = (\gamma RT_0)^{\frac{1}{2}} \approx 90$ m/s. The four basic hydrodynamic solutions discussed in §4 were computed, and the linear combination that produces maximum separative work was then determined from linearly combining the four solutions. For this calculation the hole in the top baffle was one scale height in width centred four scale heights from the rotor wall. The results are presented in Table 2.

The idealized maximum separative work available in a centrifuge is discussed in many references (e.g. Hoglund *et al.* 1979) and is given by the formula

$$\delta U(\max) = \tfrac{1}{2}\pi LcD\left(\frac{\Delta M V^2}{2RT}\right)^2, \tag{5.4}$$

where L is the length, c is the molar density, D is the diffusion coefficient, ΔM is the

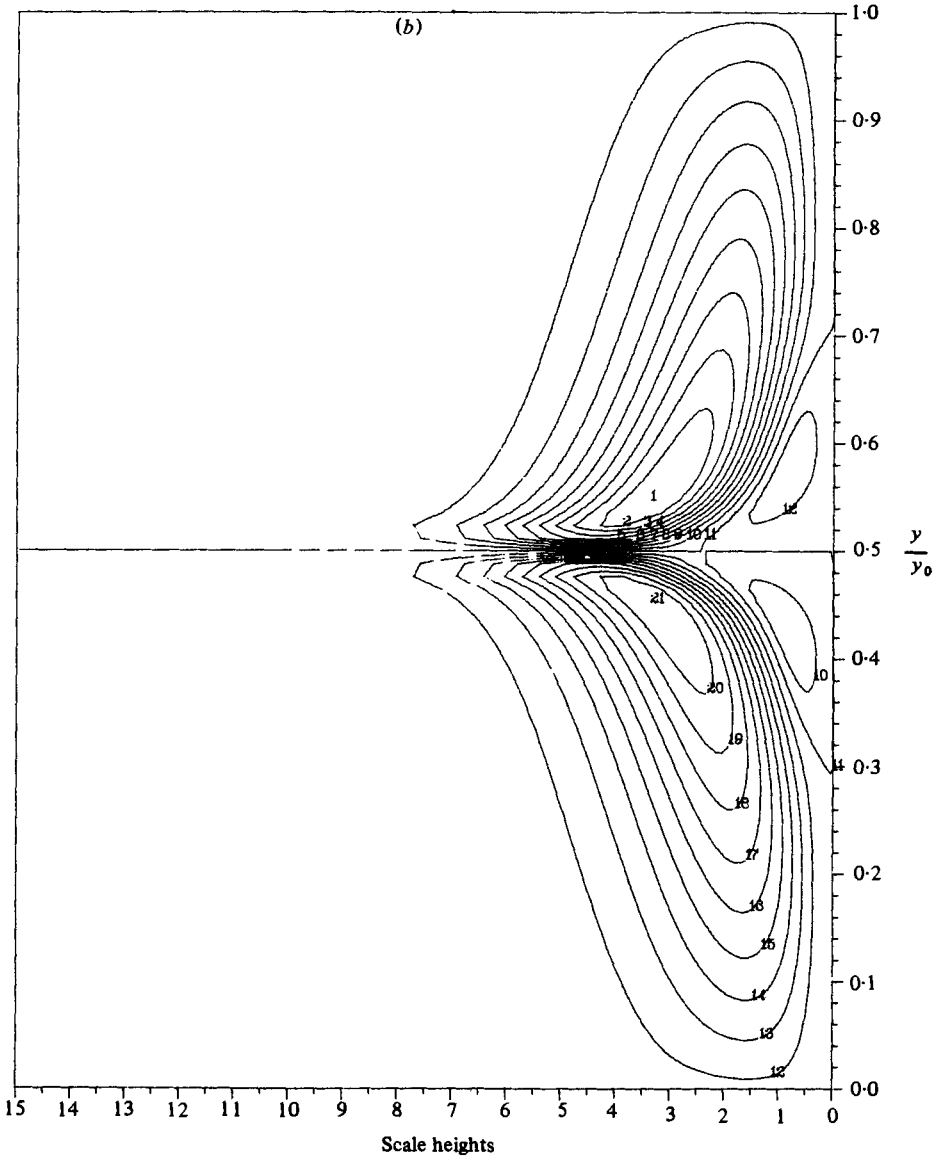

FIGURE 4(*b*). For caption see p. 310.

molecular-weight difference, V is the peripheral velocity, R is the universal gas constant and T is the temperature. Based on this equation, the efficiency can be defined as

$$E = \frac{\delta U(\text{actual})}{\delta U(\text{max})}, \tag{5.5}$$

where δU(actual) can be either the measured or predicted separative work. For the example we have calculated $E = 0{\cdot}18$.

In summary, we have shown how the model of the gas-centrifuge fluid dynamics can be coupled with the gradient equation for the isotope distribution of species. Furthermore, we have shown how the different countercurrent drive mechanisms can be modelled using sources, sinks and boundary conditions. Finally, we have indicated

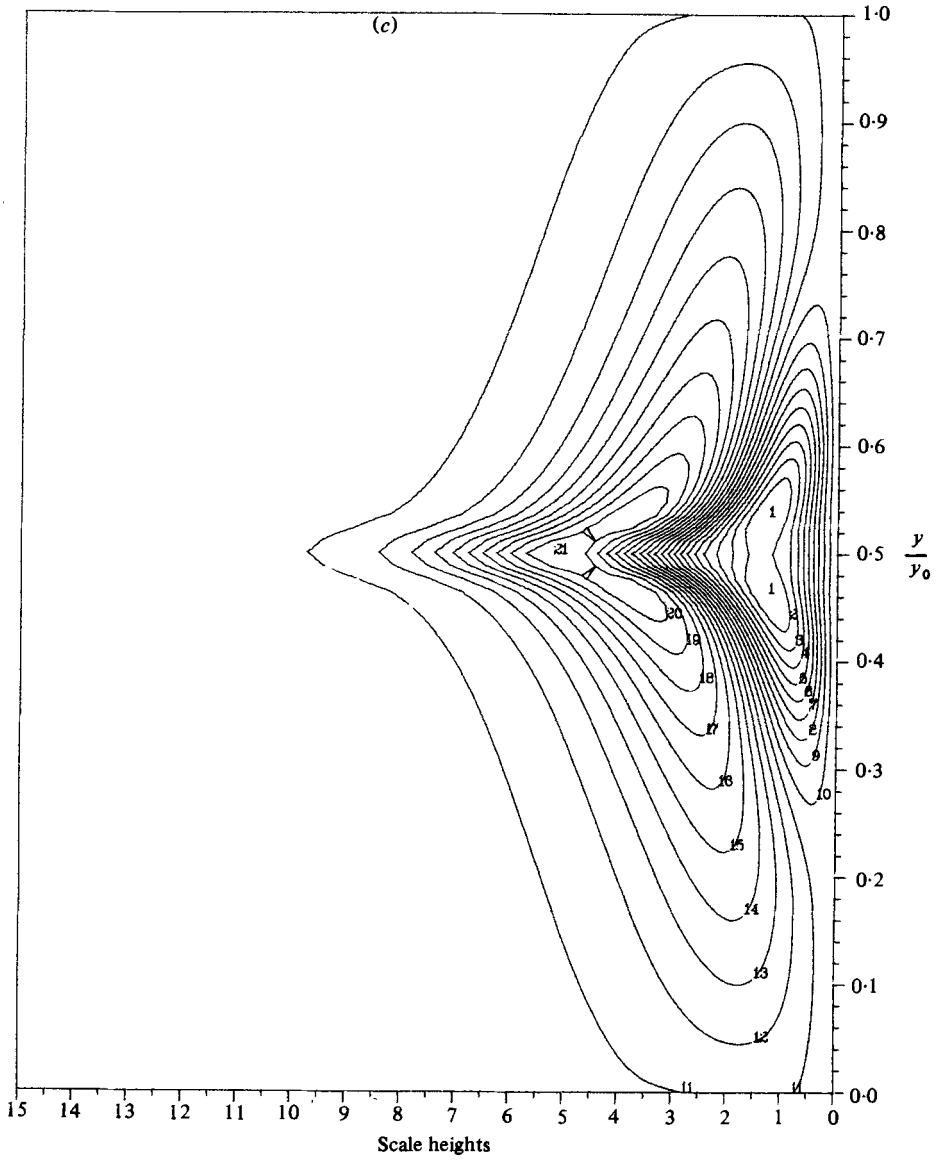

FIGURE 4. Streamlines for flow induced by (*a*) a radial-momentum source, (*b*) an angular-momentum source and (*c*) an axial-momentum source, all at $x = 8$, $y = \frac{1}{2}y_0$.

Separative work (kgU/yr)	38·6
Feed rate (mg/s)	13·2
Cut (product/feed)	0·38
Temperature difference (K)	8·0
Scoop drag (dyn)	438·0

TABLE 2. Results of separative work calculations

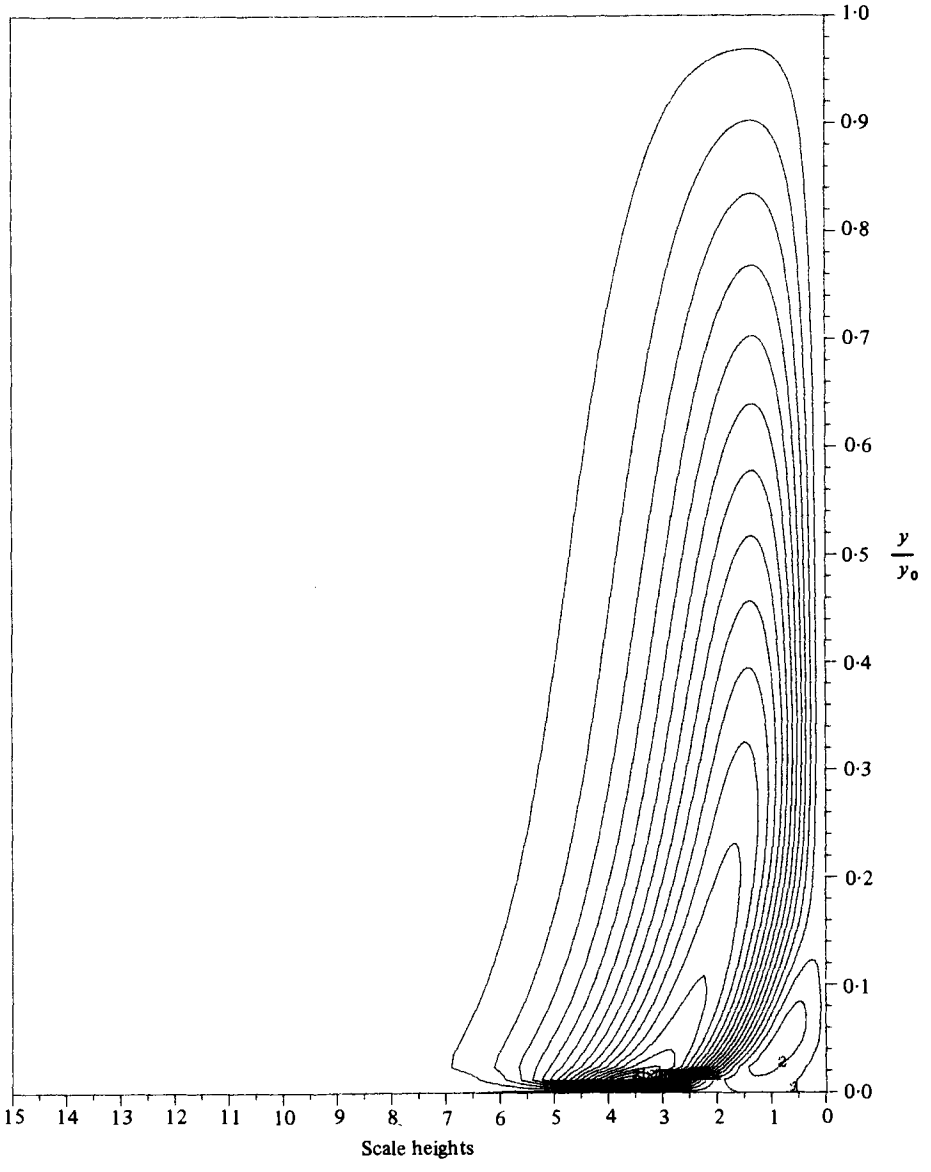

FIGURE 5. Streamlines for flow induced by a sink of angular momentum simulating the action of the bottom scoop.

how these different drive mechanisms can be combined to produce an optimum separative work based on the fluid-dynamics solutions.

The authors would like to recognize the contribution of Dr R. A. Gentry and his co-workers at Los Alamos National Laboratory, who first suggested the use of internal sources and sinks to model the action of scoops and feed. The suggestion was made in 1973. The work described in this paper was carried out for the U.S. Dept of Energy under U.S. Government Contracts W-7405 eng 26 and DE-AC05-760R01779.

Appendix A. A smoothing procedure for delta-function sources

From the discussion in §3 it should be clear that some restrictions must be placed on the source distribution. In order to be admissible functions, the source distributions must allow the necessary differentiation and integration to produce $\sigma(x)$ and $\eta(y)$. However, with some additional analysis, delta functions can be used. A smoothing procedure suggested by J. W. Painter (1977, private communication) can be used to invert the differential operator and avoid computational difficulties.

Recall that the eigenfunctions $f_n(x)$ satisfy the differential equation

$$Lf_n \equiv (e^x(e^x f_n'')'')' = -\lambda_n^2 f_n, \tag{A 1}$$

where $\lambda_n = \alpha_n B$. Using this equation to replace $f_n(x)$ in (3.10) and unfolding the differential operator with five integrations yields

$$\sum_{n=1}^{\infty} \{f_n(x) - L_4 f_n(0)\,[h_3'(x) + h_p'(x)] - L_3 f_n(0)\,[h_3'(x) + 2h_p'(x)\}\frac{a_n}{\lambda_n^2} = \bar{G}(x), \tag{A 2}$$

where

$$\bar{G}(x) = -\frac{F_0}{2B^2}\int_0^x e^{-x_1}\int_0^{x_1}\int_0^{x_2} e^{-x_3}\int_0^{x_3}\int_0^{x_4}\sigma(x_5)\,dx_5\,dx_4\,dx_3\,dx_2\,dx_1, \tag{A 3}$$

and $h_3(x)$ and $h_p(x)$ are the zero eigenfunctions discussed in WM. The values of $L_4 f_n(0)$ and $L_3 f_n(0)$ are not determined by the boundary conditions but can be determined as part of the unknown coefficients. Equation (A 2) can be rewritten as

$$\sum_{n=1}^{\infty}\frac{a_n}{\lambda_n^2} f_n'(x) - A_1 h_3'(x) - A_2 h_p'(x) = \bar{G}(x). \tag{A 4}$$

Since $f_n'(\infty) = L_3 f_n(\infty) = 0$, A_1 and A_2 can be determined by requiring

$$-A_1 h_3'(\infty) - A_2 h_p'(\infty) = \bar{G}(\infty), \tag{A 5a}$$

$$-A_1 L_3 h_3(\infty) - A_2 L_3 h(\infty) = [e^x \bar{G}'(x)]'_{x=\infty} \equiv D(\infty). \tag{A 5b}$$

The method of least squares can be applied to (A 4) to determine the coefficients a_n. Another integration can be performed on (A 4), but no significant computational advantages are gained.

For the case discussed earlier, where a source of axial momentum is considered, (3.6) shows that

$$\sigma(x) = (e^x G(x))_{xx},$$

where $G(x)$ is the radial distribution function. From (A 3), for this case

$$\bar{G}(x) = -\frac{F_0}{2B^2}\int_0^x e^{-x_1}\int_0^{x_1}\int_0^{x_2} G(x_3)\,dx_3\,dx_2\,dx_1, \tag{A 6}$$

where the condition $G'(0) = G(0) = 0$ has been imposed.

By using this smoothing procedure, we can compute the flow generated by an impulse of axial momentum acting on the ambient case of solid-body isothermal flow. In particular we assume

$$W(x, y) = S_0\,\delta(x - x^*)\,H(y). \tag{A 7}$$

Taking fewer than five integrations of (3.10) does not produce sufficient smoothing for producing good numerical results. In particular, for (A 5b), the integral in (A 6) then provides

$$D(x) = -\frac{F_0}{2B^2}\int_0^x G(x_1)\,dx_1, \tag{A 8}$$

which yields the necessary smoothing.

REFERENCES

COHEN, K. 1951 *Theory of Isotope Separation.* McGraw-Hill.

DURIVAULT, J. & LOUVET, P. 1976 Etude théorique de l'écoulement dans une centrifugeuse à contre courant thermique. *Centre D'Etudes Nucléaires de Saclay, Rapport* CEA-R-4714.

FURRY, W. H., JONES, R. C. & ONSAGER, L. 1939 On the theory of isotope separation by thermal diffusion. *Phys. Rev.* **55**, 1083.

GUNZBURGER, M. D. & WOOD, H. G. 1980 Finite element methods for the Onsager pancake equation. *Union Carbide Corp., Nucl. Div., Oak Ridge, Tennessee, Rep.* K/TS-10,274. To appear in *Comp. Meth. in Appl. Mech. Engng.*

HOGLUND, R. L., SHACTER, J. & VON HALLE, E. 1979 Diffusion separation methods. In *Encyclopedia of Chemical Technology*, vol. 7, 3rd edn (ed. R. E. Kirk & D. F. Othmer). Wiley.

MAY, W. G. 1977 Separation parameters of gas centrifuges. *A.I.Ch.E. Symp. Series* **73**, no. 169.

OLANDER, D. R. 1972 Technical basis of the gas centrifuge. *Adv. Nucl. Sci. Tech.* **6**, 105.

PARK, J. E. 1981 Calculation of the isotope distribution in a gas centrifuge. *Union Carbide Corp. Nucl. Div., Oak Ridge, Tennessee, Rep.* K/CSD/TM-36.

SOUBBARAMAYER 1979 Centrifugation. In *Uranium Enrichment* (ed. S. Villani). Topics in Applied Physics, vol. 35. Springer.

SOUBBARAMAYER & BILLET, J. 1980 A numerical method for optimizing the gas flow field in a centrifuge. *Comp. Meth. in Appl. Mech. Engng* **24**.

WOOD, H. G. & MORTON, J. B. 1980 Onsager's pancake approximation for the fluid dynamics of a gas centrifuge. *J. Fluid Mech.* **101**, 1.